

A CUBIC STRAIN QUADRILATERAL FINITE ELEMENT

A. EL-HAMALAWI*, M. D. BOLTON AND A. M. BRITTO

Engineering Department, University of Cambridge, Trumpington Street, Cambridge CB2 1PZ, U.K.

SUMMARY

In this paper, a fourth-order displacement (cubic strain) Serendipity quadrilateral element is presented. The shape functions and integration scheme are introduced, followed by a series of convergence tests, indicating that the element does not have any spurious zero-energy modes, and passes the patch test and single-element tests. Modifications are then made to enable the element's use in effective stress analysis problems. Examples are finally solved using the element and a comparison is made between some computed and closed-form solutions. It is also shown that the cubic strain quadrilateral may be used in conjunction with or as a substitute for the cubic strain triangle¹ when predicting collapse loads for undrained plane or axisymmetric problems in the fully plastic range.

KEY WORDS: cubic-strain quadrilateral; predicting collapse-loads

1. INTRODUCTION

In geotechnical engineering problems involving plasticity, the prediction of collapse loads using low-order elements has been known to create numerical problems, such as overestimating the failure load (locking) or in some cases not reaching a failure load (e.g. Nagtegaal *et al.*² Sloan³ and Toh and Sloan⁴). A strong test for collapse in highly constrained problems is to compare with analytical solutions for the footing problem. Sloan³ concluded that a suitable element to predict the collapse load was the cubic strain triangle. However, in some situations it would be efficient to use quadrilateral elements rather than triangles in regions outside the main focus of interest, in order to minimise the number of elements and nodes. The cubic strain quadrilateral with reduced integration is thus explored and is shown to behave properly.

2. CUBIC STRAIN QUADRILATERAL CHARACTERISTICS

2.1. Derivation of the shape functions

It was decided to use the Serendipity family of elements rather than Lagrange elements, due to the former elements requiring 17 nodes rather than 25, which would decrease the cost of calculations in terms of computer time, memory and backing store usage. The shape functions for the 17-noded cubic strain quadrilateral element are shown below in terms of the local coordinates ξ and η , where the node numbers are depicted in Figure 1. The general shape function

*Author to whom correspondence should be addressed.

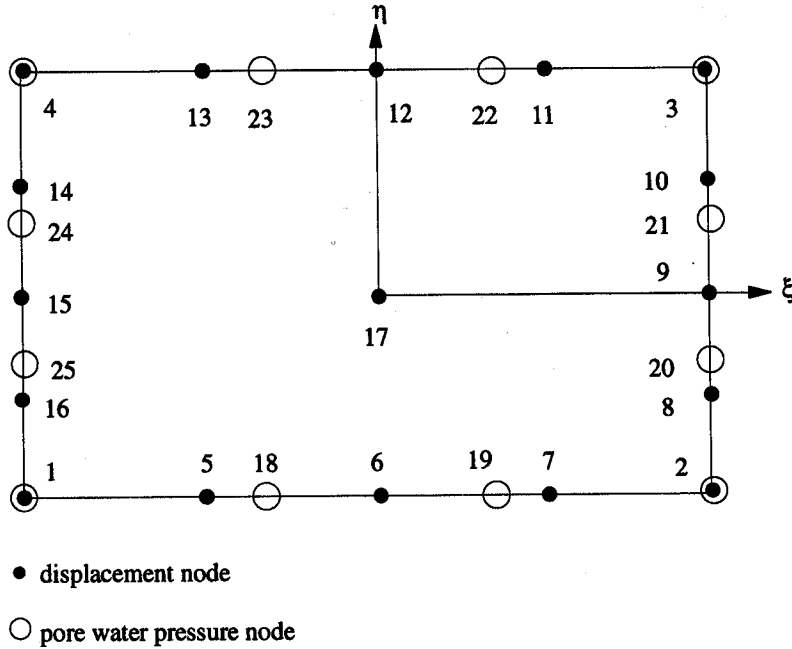


Figure 1. The effective stress analysis element with pore pressure nodes superimposed

for any node i in the element is as follows, and is detailed below for the 17 nodes:

$$N_i = \alpha_1 + \alpha_2 \xi + \alpha_3 \eta + \alpha_4 \xi^2 + \alpha_5 \xi \eta + \alpha_6 \eta^2 + \alpha_7 \xi^3 + \alpha_8 \xi^2 \eta + \alpha_9 \xi \eta^2 + \alpha_{10} \eta^3 + \alpha_{11} \xi^4 + \alpha_{12} \xi^3 \eta + \alpha_{13} \xi^2 \eta^2 + \alpha_{14} \xi \eta^3 + \alpha_{15} \eta^4 + \alpha_{16} \xi^4 \eta + \alpha_{17} \xi \eta^4 \quad (1)$$

The intermediate edge nodes are located at quarter-points along the element boundary. Serendipity elements are the most efficient elements up to third-degree polynomial approximations.⁵ Any order of element higher than three will have the element polynomial being incomplete, which means that for the cubic strain element to obtain a higher-order completeness, an interior central node has to be introduced. This is adopted in preference to the use of a nodeless function to make the element less sensitive to non-rectangularity, curvature of sides and to the placing of side nodes.⁶

$$N_1 = -1/12(-1 + \eta)(-1 + \xi)(4\xi^3 - 3\xi\eta - 4\xi + 4\eta^3 - 4\eta)$$

$$N_2 = -1/12(-1 + \eta)(1 + \xi)(4\xi^3 - 3\xi\eta - 4\xi - 4\eta^3 + 4\eta)$$

$$N_3 = 1/12(1 + \eta)(1 + \xi)(4\xi^3 + 3\xi\eta - 4\xi + 4\eta^3 - 4\eta)$$

$$N_4 = 1/12(1 + \eta)(-1 + \xi)(4\xi^3 + 3\xi\eta - 4\xi - 4\eta^3 + 4\eta)$$

$$N_5 = 2/3\xi(-1 + \xi)(2\xi - 1)(1 + \xi)(-1 + \eta)$$

$$N_6 = -1/2(-1 + \eta)(-1 + \xi)(1 + \xi)(\eta + 4\xi^2)$$

$$N_7 = 2/3\xi(-1 + \xi)(2\xi + 1)(1 + \xi)(-1 + \eta)$$

$$\begin{aligned}
N_8 &= -2/3\eta(-1 + \eta)(2\eta - 1)(1 + \eta)(1 + \xi) \\
N_9 &= -1/2(-1 + \eta)(1 + \eta)(1 + \xi)(\xi - 4\eta^2) \\
N_{10} &= -2/3\eta(-1 + \eta)(2\eta + 1)(1 + \eta)(1 + \xi) \\
N_{11} &= -2/3\xi(-1 + \xi)(2\xi + 1)(1 + \xi)(1 + \eta) \\
N_{12} &= 1/2(1 + \eta)(-1 + \xi)(1 + \xi)(-\eta + 4\xi^2) \\
N_{13} &= -2/3\xi(-1 + \xi)(2\xi - 1)(1 + \xi)(1 + \eta) \\
N_{14} &= 2/3\eta(-1 + \eta)(2\eta + 1)(1 + \eta)(-1 + \xi) \\
N_{15} &= -1/2(-1 + \eta)(1 + \eta)(-1 + \xi)(\xi + 4\eta^2) \\
N_{16} &= 2/3\eta(-1 + \eta)(2\eta - 1)(1 + \eta)(-1 + \xi) \\
N_{17} &= (1 - \xi^2)(1 - \eta^2)
\end{aligned} \tag{2}$$

2.2. Integration scheme

The method of integration commonly used with finite elements to evaluate the stiffness matrix is the Gauss–Legendre quadrature. Zienkiewicz and Taylor⁷ state that no loss of convergence occurs providing the integration is exact to the order of $2(p - m)$, or shows an error of order $O(h^{2(p-m)+1})$, where p is the degree of the complete polynomial present and m is the order of differentials occurring in the problem. For a C^0 problem, $m = 1$ and $p = 4$ for a cubic strain element leading to an error of order $O(h^7)$. This in turn means that ‘full integration’ may be accomplished by using a 5×5 integration rule. However, a lower-order quadrature (4×4 integration rule) called *reduced integration* will be used. Sloan³ predicted that for a cubic strain quadrilateral in plastic undrained axisymmetric problems, full integration would cause locking. With reduced integration, the constraint ratio (equal to the ratio of degrees of freedom per element and constraints per element) would become equal to unity, thus avoiding locking. Another justification is that the error introduced by the inexact evaluation of the stiffness matrices is approximately balanced by the error due to inadequate discretisation,⁶ and the computational cost in terms of time overhead to integrate over 16 sampling points is less than integrating 25 points in a full integration.

3. ASSESSMENT OF ELEMENT CONVERGENCE

The two main convergence criteria for an element involve checking the *consistency* and the *stability* conditions of an element. The former criterion ensures that the error decreases and tends to zero as the element size is reduced, and that the finite element approximate equations will represent the exact differential equation and the boundary equations.⁷ The stability condition however checks that no zero-energy modes exist in the element and that the solution obtained is a unique one. The latter condition has been checked using the eigenvalue test.

The first patch test constituted choosing a ‘patch’ of four rectangular elements with one internal node in the middle and four interelement boundaries. Displacements corresponding to an arbitrary state of constant stress were then imposed on the boundary of the patch, and the displacements at the internal node resulting from the finite element analysis correlated *exactly* with the applied displacement field, resulting in a constant state of strain and stress throughout the patch.

A second test was performed on a different patch which included an element of irregular shape, and the previous procedure re-applied with the same displacement field. The main reason for this second test was the fact that some elements pass the patch test with certain restrictive shapes such as rectangles or parallelograms.⁸ The nodal co-ordinates and the resulting displacements were in exact agreement with the applied displacement field, along with the strains and stresses being constant, thus confirming the consistency of the element in question.

The eigenvalue test ensures the stability of the element in question by detecting any zero-energy deformation modes and lack of rigid-body motion capability. It is especially important to perform this test since reduced integration is being used which might cause spurious modes of deformation to occur. The element is unrestrained to provide a complete stiffness matrix. For a plane element, three of the eigenvalues should be equal to zero, corresponding to the three rigid-body modes. Any other eigenvalue that is equal to zero would indicate the presence of an instability arising from one of the nodal displacement vectors not being a rigid-body motion but producing zero strain energy. The eigenvalues of the unrestrained element indicated the three 'zero eigenvalues'.

The last test undergone by the element was the single-element test. This was done since the properties displayed by an element in a mesh or patch may be different than when applying the load to the element in isolation. It thus examines the effect of distorting the element. Two states of constant stress loadings were applied to the element separately. The resulting displacements and strains at the nodes were equal to the theoretical solution. The values of the stresses throughout the element were also equal to the applied load, and the reactions at the nodes were found to be in equilibrium with the applied loading. The side at which the load was applied was also found to remain straight.

4. EXTENSION TO EFFECTIVE STRESS ANALYSIS

For the case of the cubic strain element being used in consolidation, a lower order (by one order) of quadrilateral is used to represent the pore water pressures; the quadratic strain quadrilateral. This is due to the pore pressures being of the same order of variation as the variation in strain, which is given by the first derivative of the displacement functions. The shape functions of the quadratic strain quadrilateral may be found in Reference 9. The corner nodes will have three degrees of freedom (u, v, σ_{pp}), with three intermediate nodes having two degrees of freedom (u, v) and two intermediate nodes having one degree of freedom (σ_{pp}) on each side of the quadrilateral, as shown in Figure 1. The element has been tested for a one-dimensional Terzaghi consolidation problem in Section 5.1.

5. NUMERICAL EXAMPLES

In the numerical examples that follow, the critical state soil mechanics package *CRISP* – 94¹⁰ was used as a platform to test the cubic strain quadrilateral element.

5.1. One-dimensional consolidation

A one-dimensional Terzaghi axisymmetric consolidation problem is analysed to demonstrate the use of the effective stress cubic strain quadrilateral element. The results are compared with the already established cubic strain triangle element.¹ One cubic strain quadrilateral element is used to solve the problem along with another mesh comprising two cubic strain triangles. The vertical

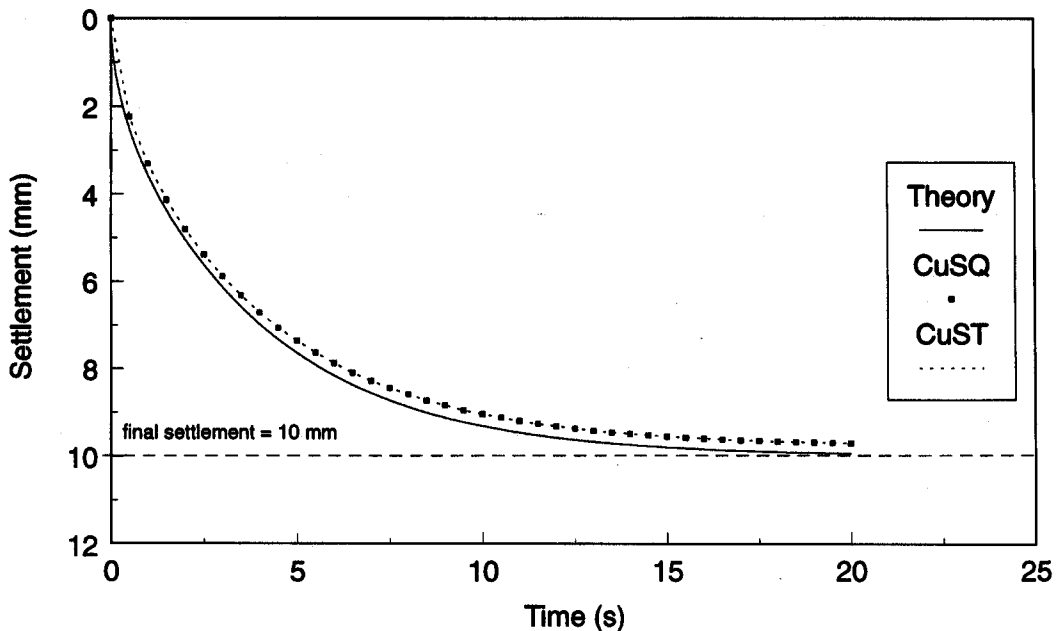


Figure 2. The settlement-time curve for the 1-D Terzaghi consolidation problem

sides and bottom of the sample are restrained and assumed to be smooth. The sample is initially unstressed, and a load of 100 kPa is applied to the top surface. The transient response of the sample under the applied load is studied over 20 s, subdivided into 0.5 s time increments (40 increments).

The results are shown in Figure 2, with the theoretical solution obtained from Taylor's Fourier solution,¹¹ given by equation (3).

$$\bar{U} = 1 - \sum_{m=1}^{\infty} \frac{2}{M^2} e^{-M^2 T_v}, \quad M = \frac{1}{2} \pi(2m - 1) \quad (3)$$

where \bar{U} is the average degree of consolidation and T_v is the time factor, given (for 'single drainage') by,

$$T_v = \frac{C_v t}{H^2} \quad (4)$$

where H is the length of the sample (1 m) and C_v is the coefficient of consolidation (equal to 10^5 mm²/s). 500 terms were used to represent the series to obtain the theoretical solution. The settlement shown in Figure 2 was calculated using

$$\rho = \rho_{\infty} \bar{U} \quad (5)$$

$$\rho_{\infty} = m_v H \sigma' = 10 \text{ mm} \quad (6)$$

where m_v is the coefficient of compressibility (equal to 10^{-7} m²/N). It can be seen in Figure 2 that a good agreement exists between the finite element analysis and the theoretical curves, with errors being in the range of 2–4 per cent.

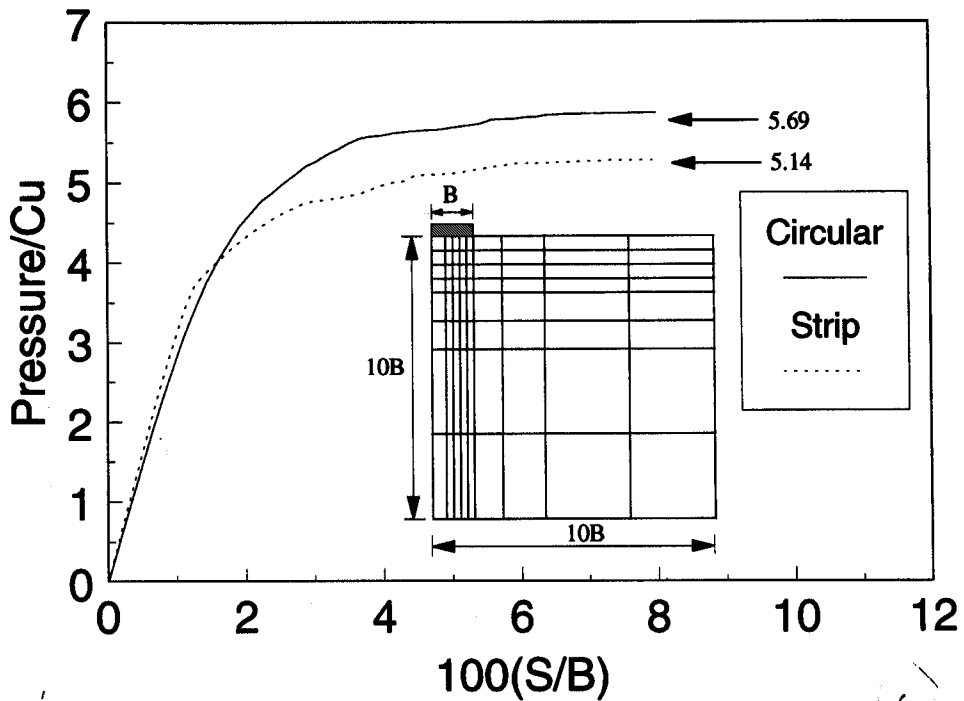


Figure 3. The deformation response of the soil due to the smooth rigid footing modelled with CuSQ elements

5.2. Rigid circular and strip footings on a cohesive undrained soil

The second problem solved was that of the collapse load of a rigid footing (plane strain and axisymmetric cases) on a cohesive undrained soil. 72 cubic strain quadrilateral elements were used to model the geometry of the problem, shown in Figure 3. Half the footing was analysed, accounting for symmetry. This problem was specifically chosen because of its testing nature with regard to the singularity that exists at the edges of the footing. As mentioned previously, it had been analysed extensively by Sloan and co-workers,^{1,3} who deduced that cubic strain triangles and quadrilaterals were suitable for the analysis of plane strain collapse load prediction problems. The same author, however, postulated that for the axisymmetric case, only the cubic strain triangle should be used since the cubic strain quadrilateral with full integration was predicted to cause 'locking', where either the collapse load is overestimated, or the solution fails to converge.

A total stress analysis using 50 imposed displacement increments and the Tresca yield criterion was employed. The soil was assumed to be weightless, homogeneous, continuous and no account of the *in situ* stresses was taken into consideration. The undrained Poisson's ratio was assumed to be equal to 0.49, the shear modulus equal to 100 times the undrained soil shear strength ($G = 100c_u$), and the undrained angles of internal friction and dilation were set equal to 0.

For the smooth rigid strip footing, Prandtl¹² derived a theoretical collapse value of $5.14c_u$. Sloan and Randolph¹ solved the same problem with 72 linear strain quadrilateral elements and 48 cubic strain triangles; the solution was captured to within 3 per cent and 1 per cent respectively. In Figure 3, it can be seen that the solution using 72 cubic strain quadrilaterals is

within 2.5 per cent of the actual value, which is acceptable, and it could have been made more accurate by using a finer mesh beneath the footing.

For the smooth rigid circular footing, Shield's¹³ theoretical collapse load was $5.69c_u$. Sloan's and Randolph's¹ solution using 72 linear strain quadrilateral elements rose at an approximately constant gradient beyond the theoretical solution and 'locked'. With 48 cubic strain triangles, Sloan's solution was within a 4 per cent error. In Figure 3, where settlement S normalised by width B of footing is plotted against pressure normalised by c_u , the solution using 72 cubic strain quadrilaterals was found to be within 3 per cent of the actual value. It can also be observed that the two curves tend to converge towards their respective terminal values, with the slope of the last portion of the curves approaching zero, indicating a stabilisation of the final collapse loads. Near the centre-line of the footing, where numerical problems usually arise, it was found that the normalized stress is only 4.5 per cent greater than at the edge of the footing; this is acceptable.

6. CONCLUDING REMARKS

A rectangular cubic strain element has been presented and shown to pass the standard patch and single-element tests. It has also been demonstrated that even though a reduced integration scheme has been used, the element does not possess any spurious modes, and the results obtained in various examples justify its use.

The extension of the element to accommodate effective stress analyses proved successful since the results computed in the consolidation example were comparable to the cubic strain triangle and theoretical solutions. Convergence in plane and axisymmetric bearing capacity tests on undrained clay was excellent, confirming that the integration scheme for the element, which decreases the maximum number of incompressibility constraints to 16 and in turn lowers the constraint ratio to one, avoids the locking problem investigated by Sloan and co-workers.^{1,3} It would therefore seem that the quartic displacement quadrilateral element is a useful addition to the tools available for finite element analysis in general, and predicting collapse loads for undrained problems in the plastic range in particular.

NOTATION

| | |
|-----------|---|
| B | width of footing |
| c_u | undrained soil shear strength |
| C_v | coefficient of consolidation |
| E | elastic modulus of elasticity |
| G | elastic shear modulus |
| h | characteristic length of an element |
| m_v | coefficient of compressibility |
| N_i | shape function |
| p | order of polynomial |
| S | settlement of the footing |
| t | time |
| T_v | time factor |
| \bar{U} | average degree of consolidation |
| u, v | displacements in the x - and y -directions respectively |

Greek letters

| | |
|---------------|-------------------------------|
| ξ, η | normalised local co-ordinates |
| ρ | settlement at time t |
| ρ_∞ | final settlement |
| σ_{pp} | pore water pressure |
| ν | Poisson's ratio |

REFERENCES

1. S. W. Sloan and M. F. Randolph, 'Numerical prediction of collapse loads using finite element methods', *Int. J. numer. Analytic. Meth. Geomech.*, **6**, 47-76 (1982).
2. J. C. Nagtegaal, D. M. Parks and J. R. Rice, 'On numerically accurate finite element solutions in the fully plastic range', *Comp. Meth. Appl. Eng.*, **4**, 153-177 (1974).
3. S. W. Sloan, 'Numerical analysis of incompressible and plastic solids using finite elements', *Ph. D. Thesis*, Engineering Department, University of Cambridge, 1981.
4. C. T. Toh and S. W. Sloan, 'Finite element analyses of isotropic and anisotropic cohesive soils with a view to correctly predicting impending collapse', *Int. J. Numer. Analytic Meth. Geomech.*, **4**, 1-23 (1980).
5. R. L. Taylor, 'On completeness of shape functions for finite element analysis', *Int. J. Numer. Methods Eng.*, **4**, 17-22 (1972).
6. R. D. Cook, D. S. Malkus and M. E. Plesha, *Concepts and Applications of Finite Element Analysis*, 3rd Edition, John Wiley, New York, 1989.
7. O. C. Zienkiewicz and R. L. Taylor, *The Finite Element Method—Vol. 1* 4th Edition, McGraw Hill, Berkshire, 1989.
8. A. Razzaque, 'The patch test for elements', *Int. J. Numer. Methods Eng.* **22**, 63-71 (1986).
9. F. L. Stasa, *Applied Finite Element Analysis for Engineers*, CBS College Publishing, New York, 1986.
10. A. M. Britto and M. J. Gunn, *CRISP-94: User's and Programmer's Guide*, Engineering Department, Cambridge University, Cambridge, 1994.
11. D. W. Taylor, *Fundamentals of Soil Mechanics*, Wiley, New York, 1948.
12. L. Prandtl, 'Über die härte plastischer körper', *Göttinger Nachrichten, Math. Phys.*, **K1**, 74-85 (1920).
13. R. T. Shield, 'On the plastic flow of metals under conditions of axial symmetry', *Proc. Roy. Soc. Lond. A.* **233**, 267 (1955).